

Electronic Supplementary Information (ESI)

Catalytic decomposition of N₂O over Rh/Zn-Al₂O₃ catalysts

Chengyun Huang,^a Zhen Ma,*^b Changxi Miao,*^c Yinghong Yue,^a Weiming Hua*^a and Zi Gao^a

^a Shanghai Key Laboratory of Molecular Catalysis and Innovative Materials, Department of Chemistry, Fudan University, Shanghai 200433, PR China

^b Shanghai Key Laboratory of Atmospheric Particle Pollution and Prevention (LAP³), Department of Environmental Science and Engineering, Fudan University, Shanghai 200433, PR China

^c Shanghai Research Institute of Petrochemical Technology SINOPEC, Shanghai 201208, PR China

E-mail addresses: zhenma@fudan.edu.cn (Z. Ma), miaocx.sshy@sinopec.com (C. Miao), wmhua@fudan.edu.cn (W. Hua).

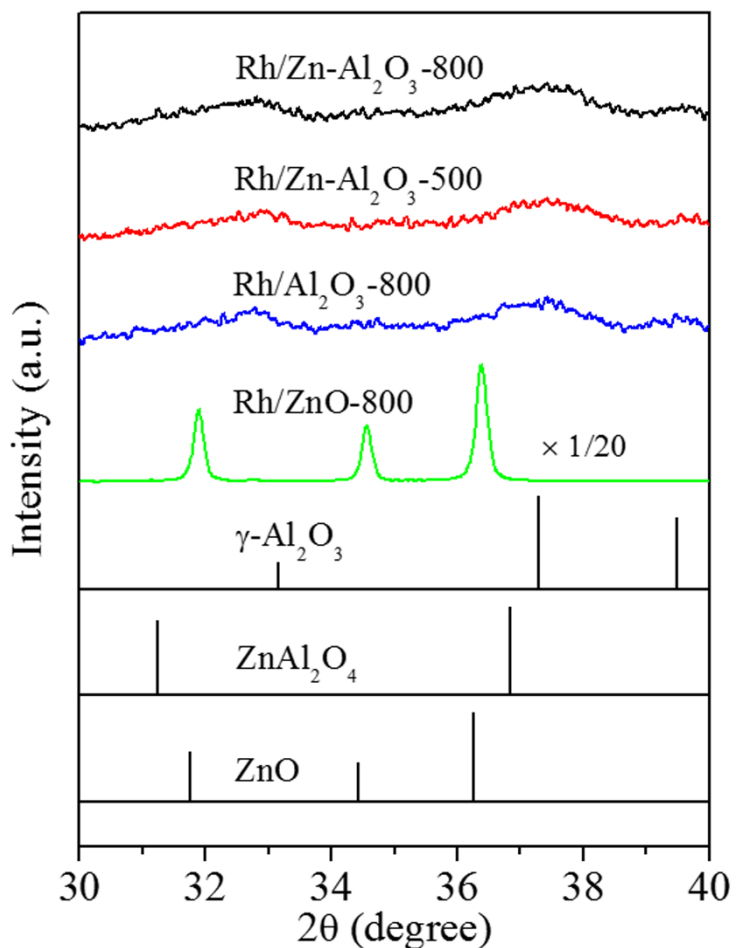


Fig. S1. XRD patterns of the catalysts and standard patterns of γ -Al₂O₃ (PDF#47-1308), ZnAl₂O₄ (PDF#05-0699), and ZnO (PDF#36-1451) in the $2\theta = 30\text{--}40^\circ$ region.

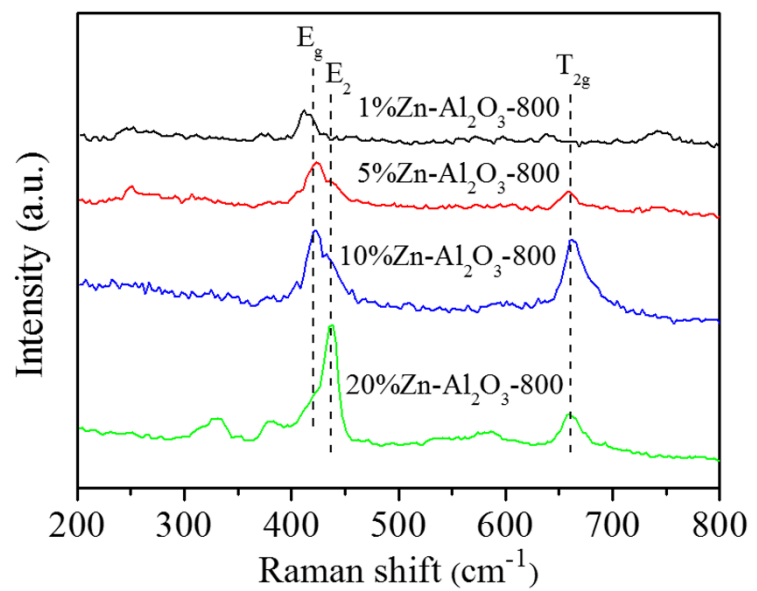


Fig. S2. Raman spectra for Zn-Al₂O₃-800 with different Zn content.

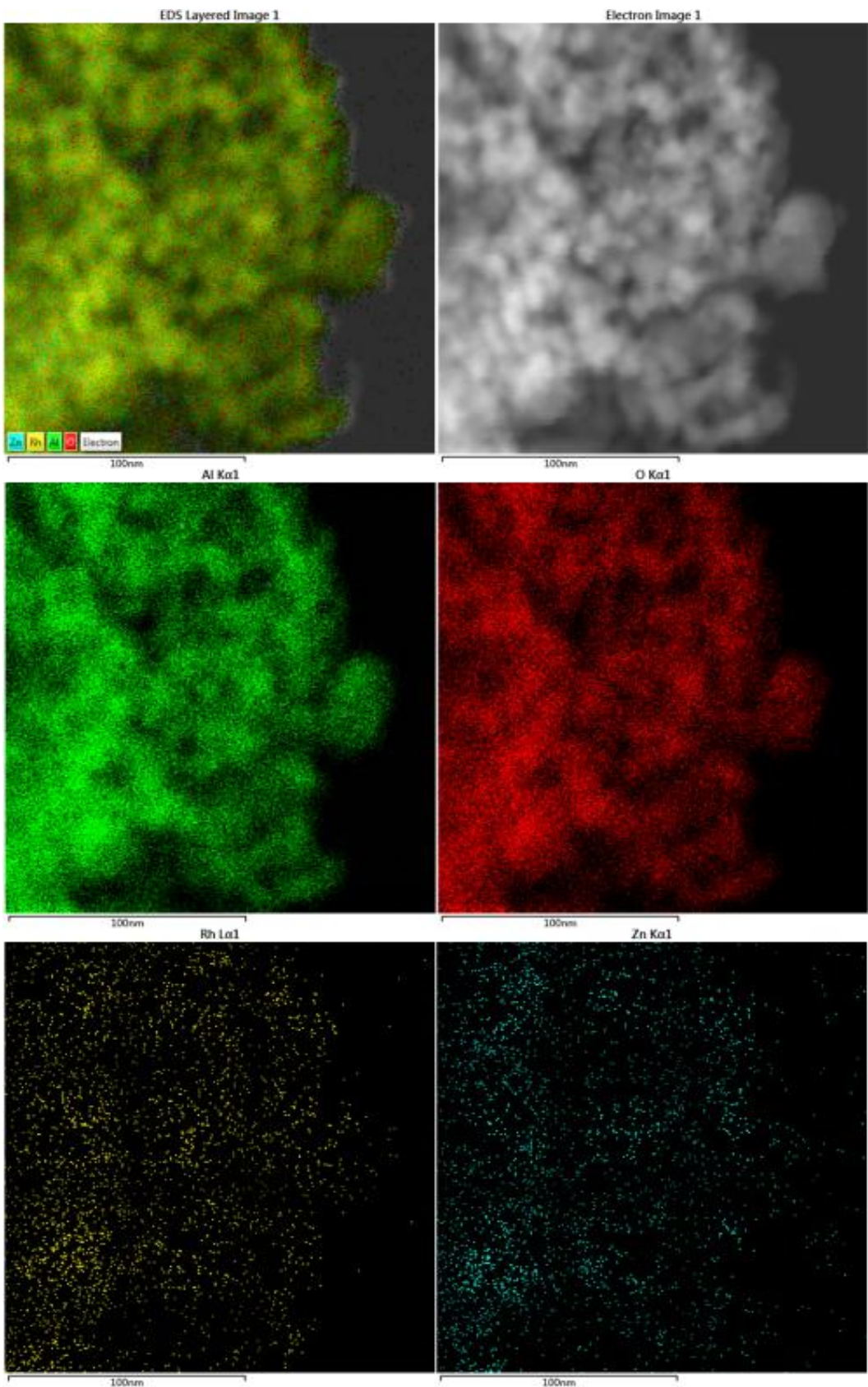
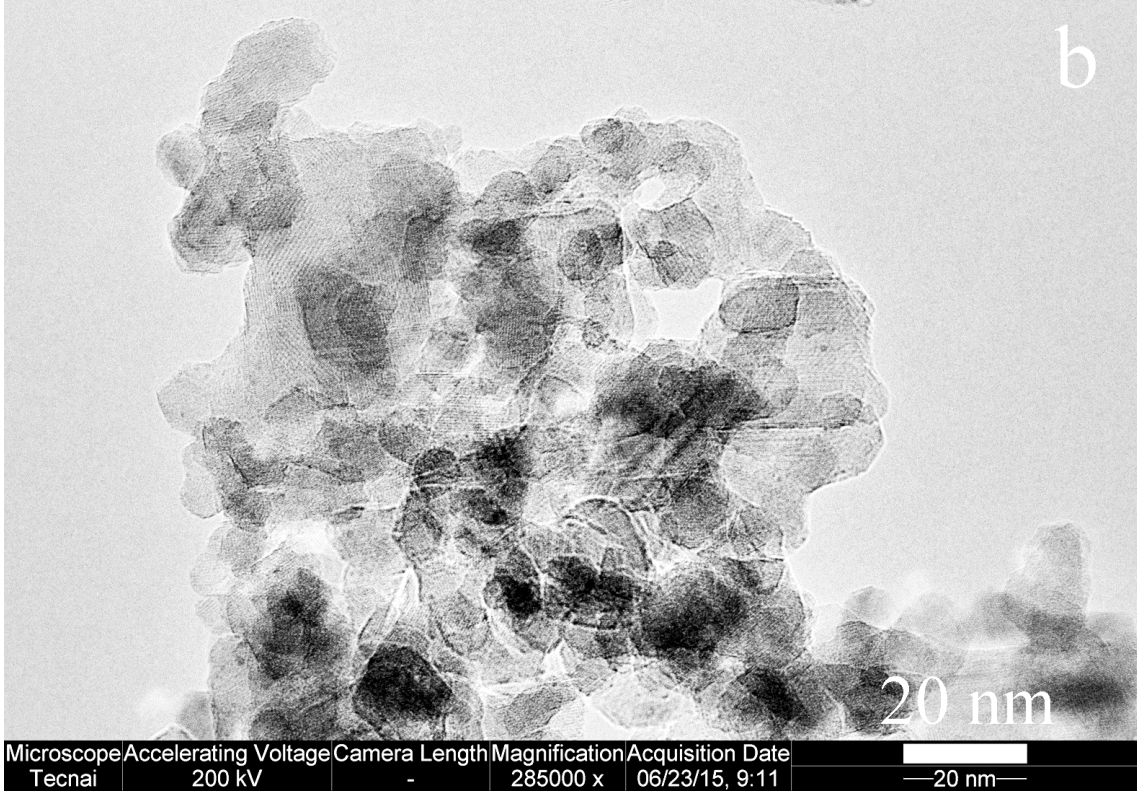
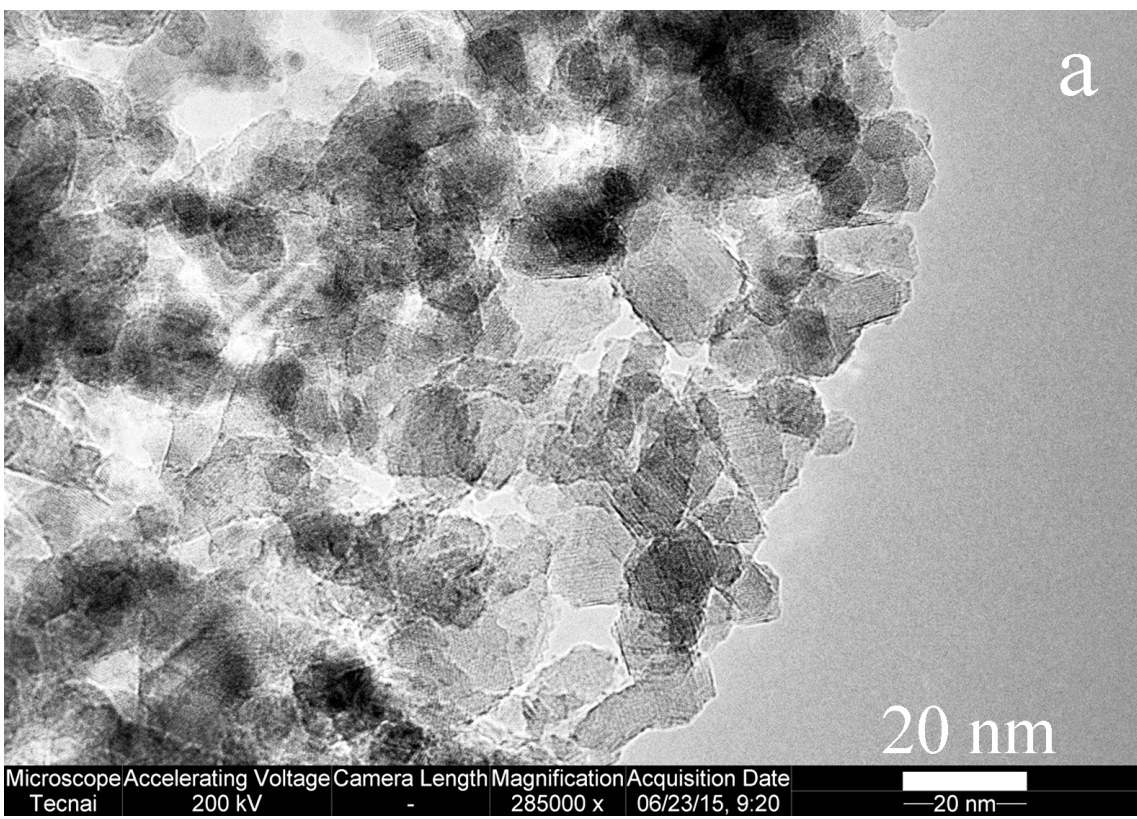


Fig. S3. EDX elemental mapping for Rh/Zn-Al₂O₃-800.



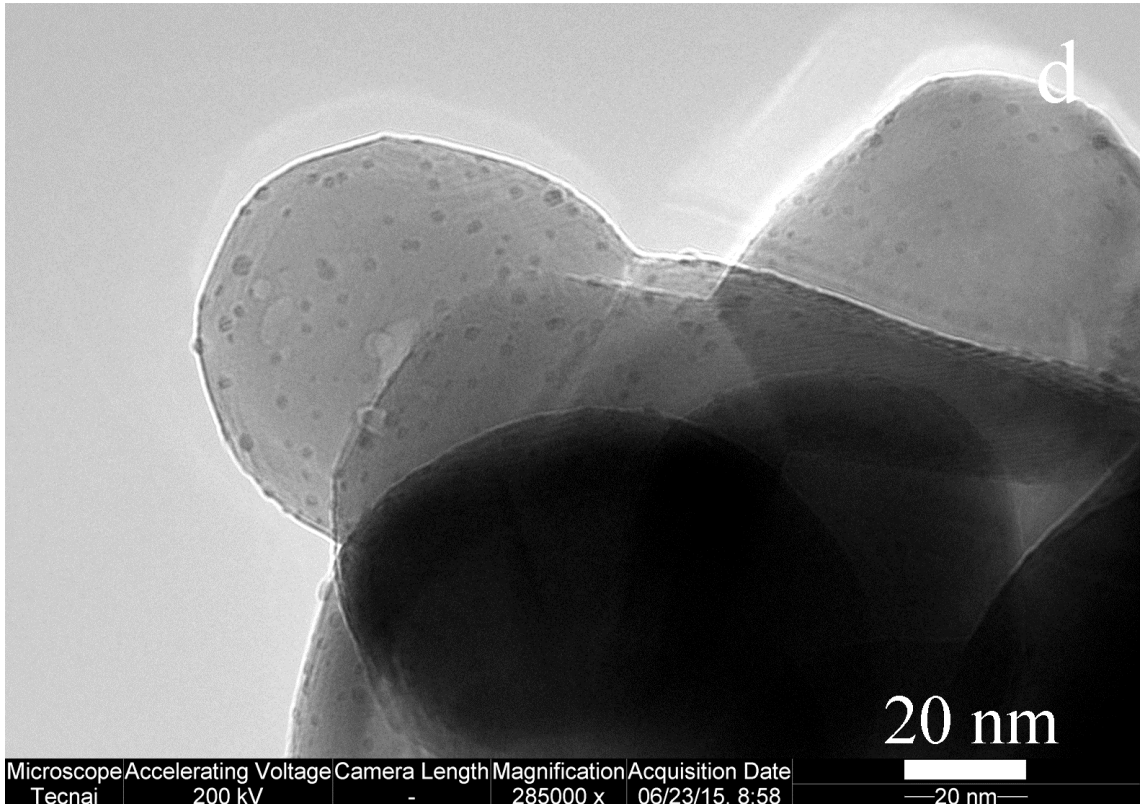
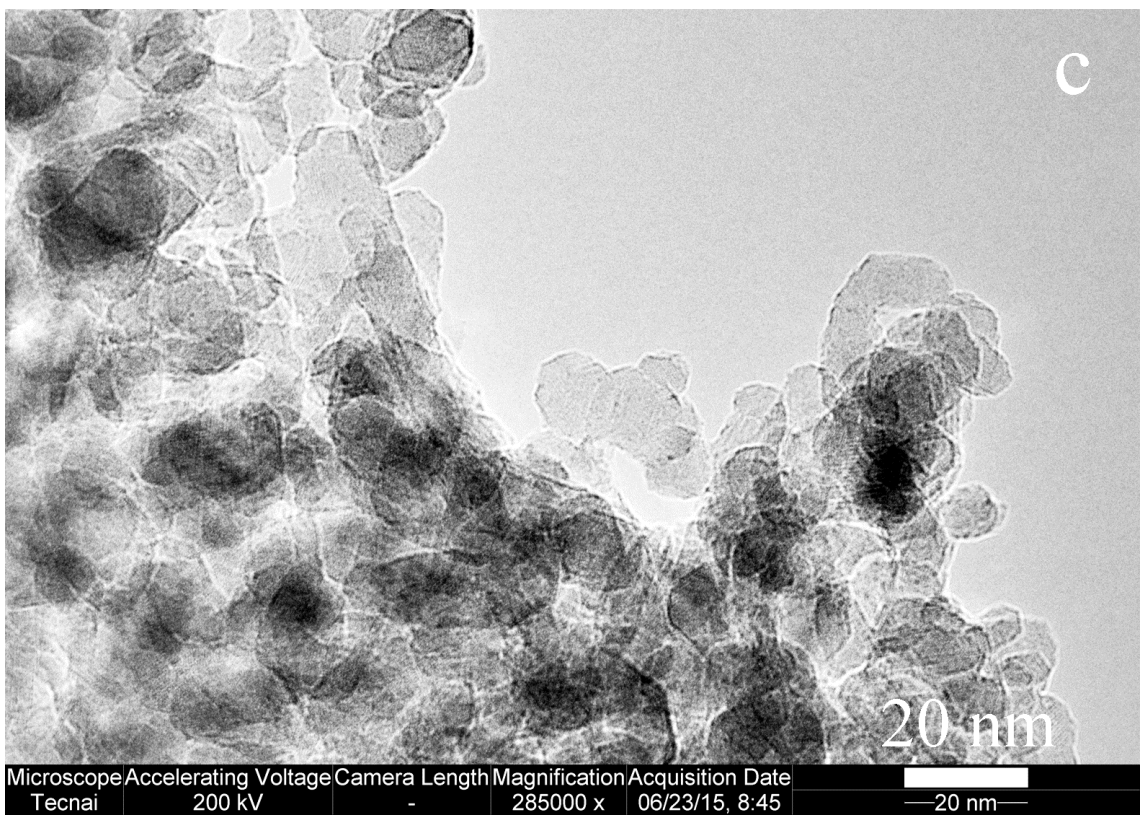


Fig. S4. TEM graphs with larger size for (a) Rh/Zn-Al₂O₃-800, (b) Rh/Zn-Al₂O₃-500, (c) Rh/Al₂O₃-800, and (d) Rh/ZnO-800.

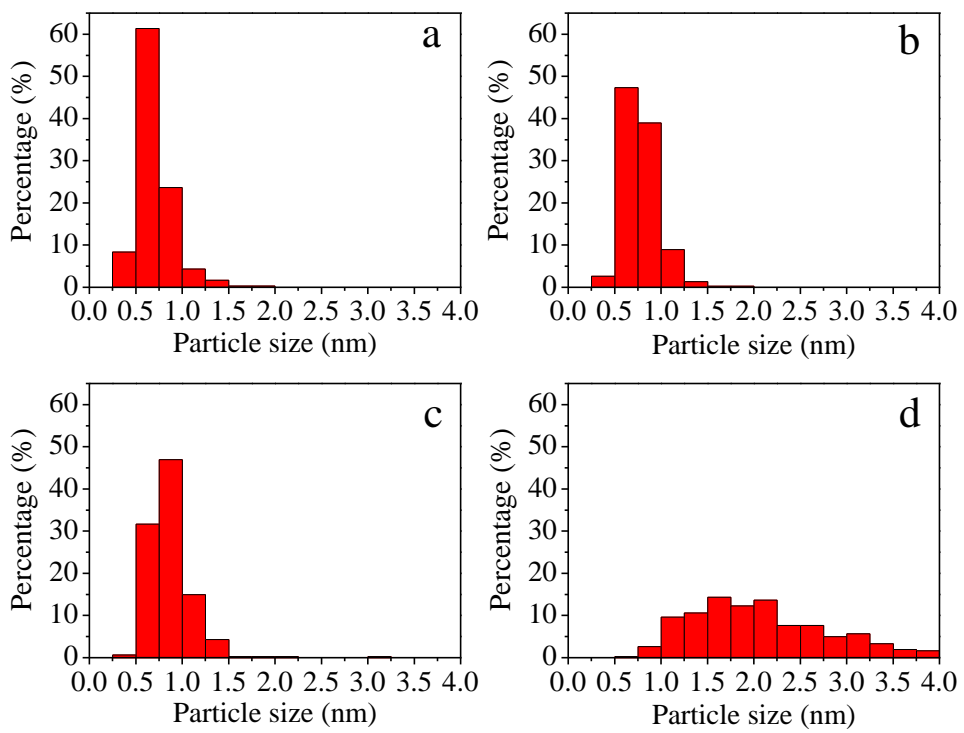


Fig. S5. Distribution of Rh_2O_3 particle sizes for (a) $\text{Rh}/\text{Zn-Al}_2\text{O}_3$ -800, (b) $\text{Rh}/\text{Zn-Al}_2\text{O}_3$ -500, (c) $\text{Rh}/\text{Al}_2\text{O}_3$ -800, and (d) Rh/ZnO -800.

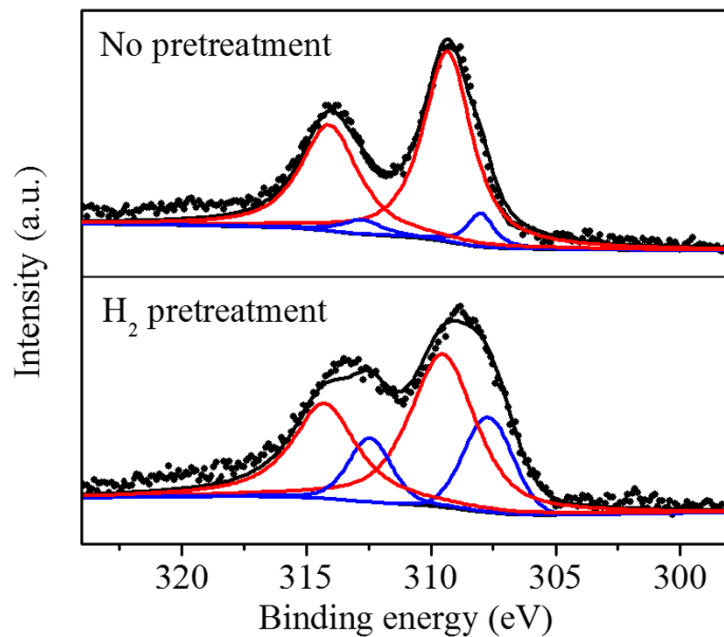


Fig. S6. Rh 3d XPS spectra of Rh/Zn-Al₂O₃-800 without being pretreated or after being pretreated in 4% H₂ (balance He) at 400 °C for 2 h.

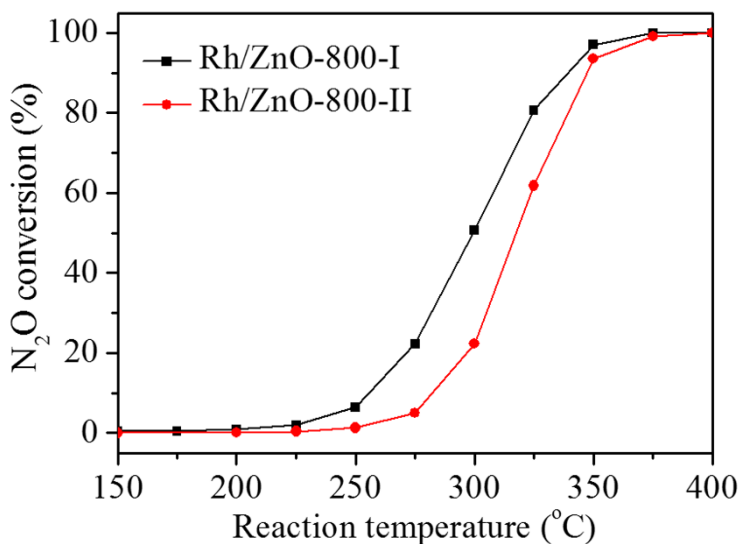


Fig. S7. Conversion of N₂O on Rh/ZnO-800 catalysts prepared using ZnO supports

prepared differently. I: ZnO support was prepared by precipitation. II: ZnO support was prepared by calcining Zn(NO₃)₂•6H₂O at 800 °C for 4 h.

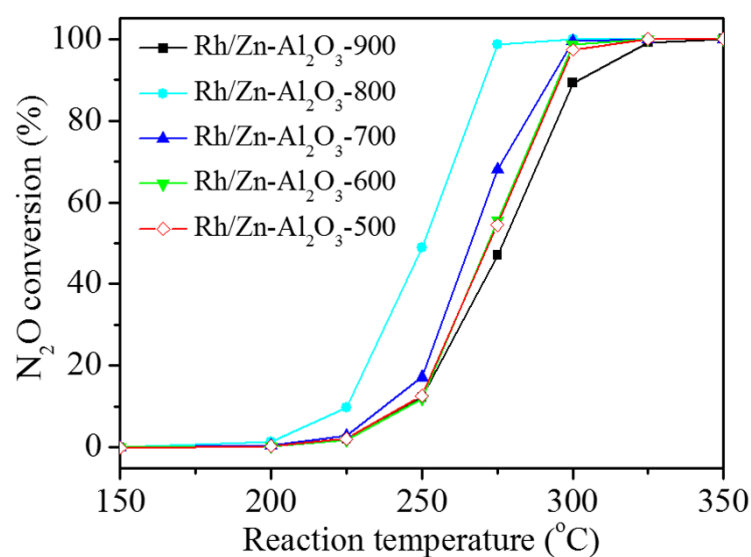


Fig. S8. Conversion of N₂O on Rh/Zn-Al₂O₃ catalysts prepared by using Zn-Al₂O₃ supports calcined at different temperatures. The loading of Zn is 1 wt%.

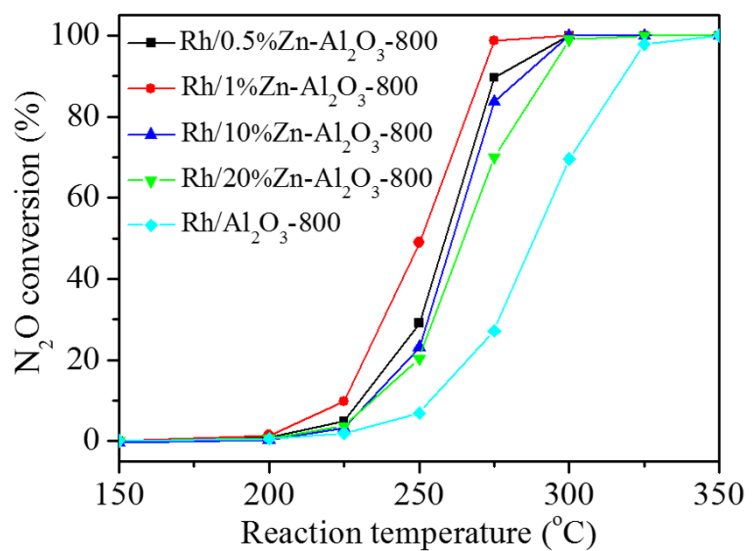


Fig. S9. Conversion of N₂O on Rh/Zn-Al₂O₃-800 catalysts with different Zn loadings.

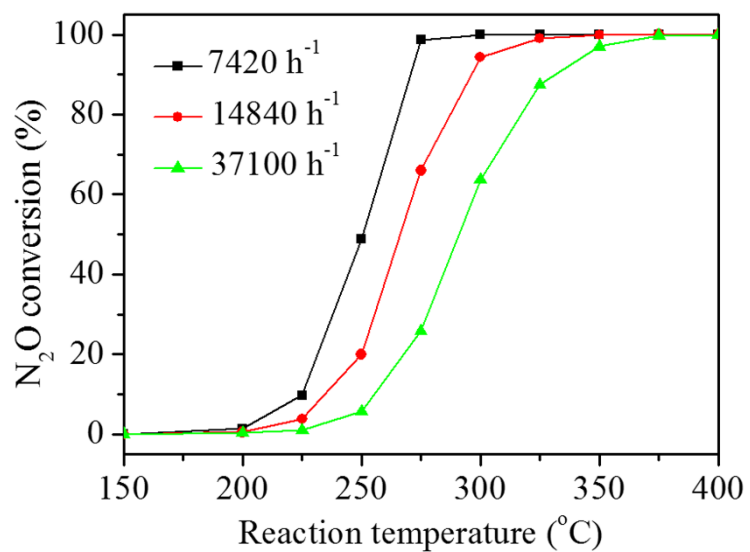


Fig. S10. Conversion of N₂O on Rh/1%Zn-Al₂O₃-800 at different GHSVs.

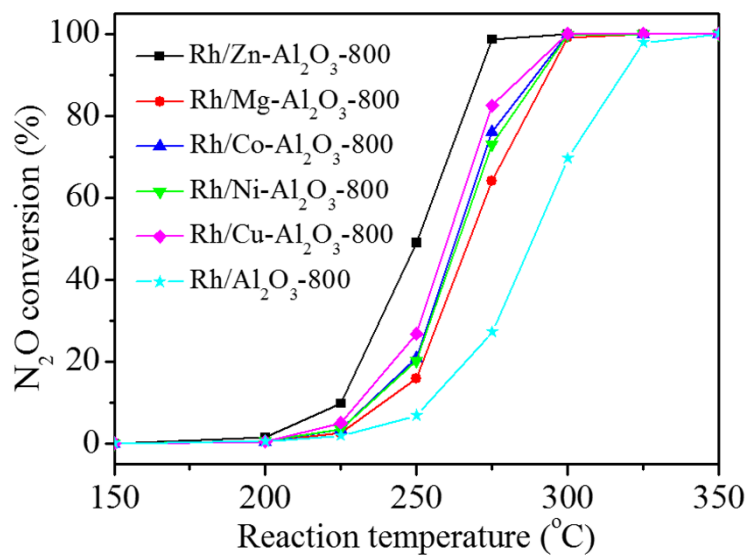


Fig. S11. Conversion of N₂O on different Rh/M-Al₂O₃-800 catalysts as a function of reaction temperature.

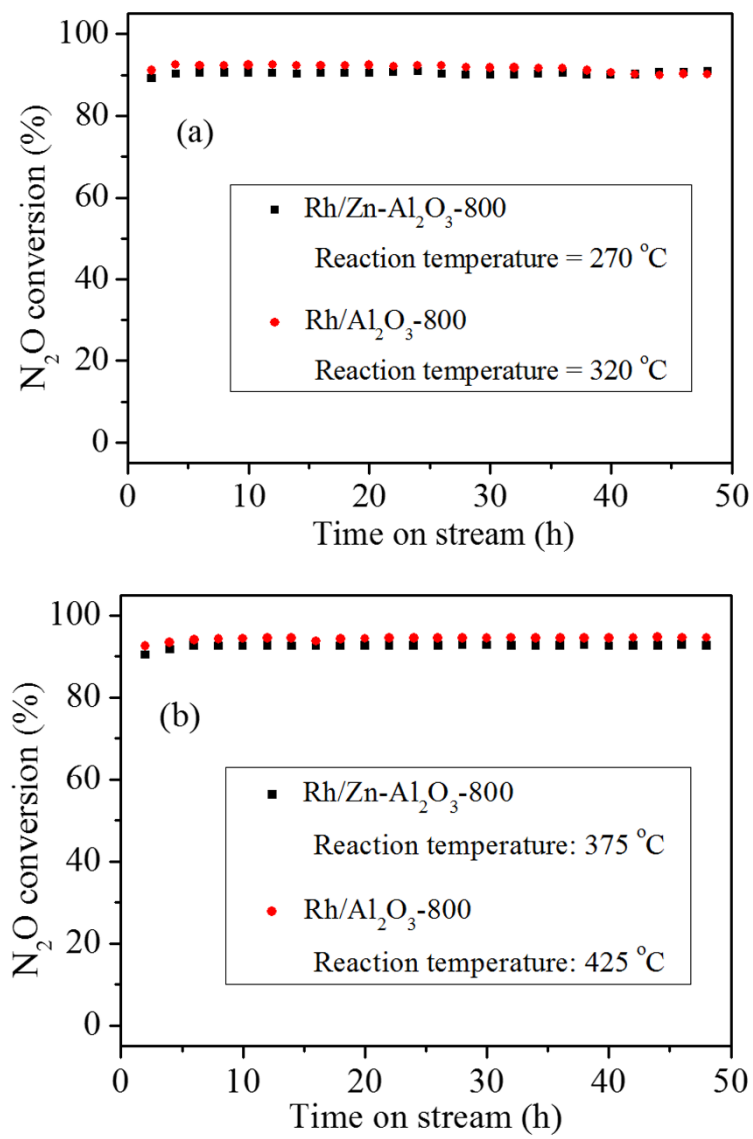


Fig. S12. Conversion of N_2O on Rh/Zn- Al_2O_3 -800 and Rh/ Al_2O_3 -800 as a function of reaction time in the flow of (a) 0.5% $\text{N}_2\text{O}/\text{He}$ and (b) 0.5% $\text{N}_2\text{O} + 2\%$ $\text{H}_2\text{O} + 5\%$ O_2/He .

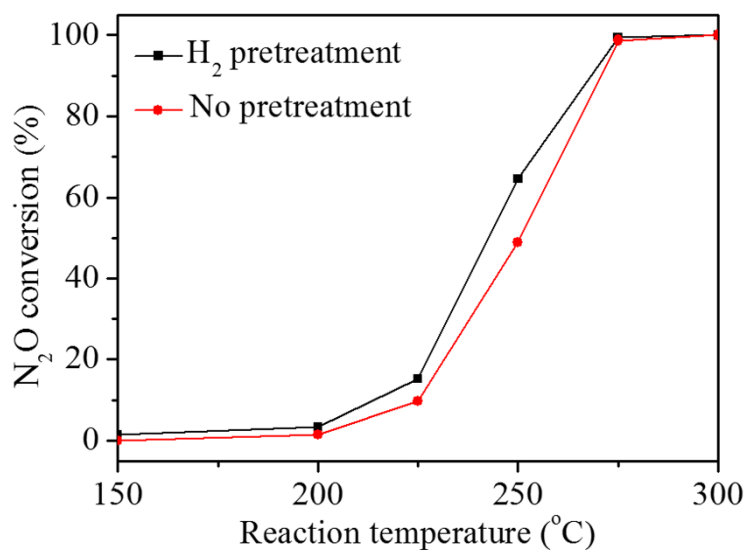


Fig. S13. Conversion of N_2O on $\text{Rh}/\text{Zn-Al}_2\text{O}_3\text{-}800$ catalyst with and without H_2 pretreatment ($400\text{ }^{\circ}\text{C}$ for 2 h).

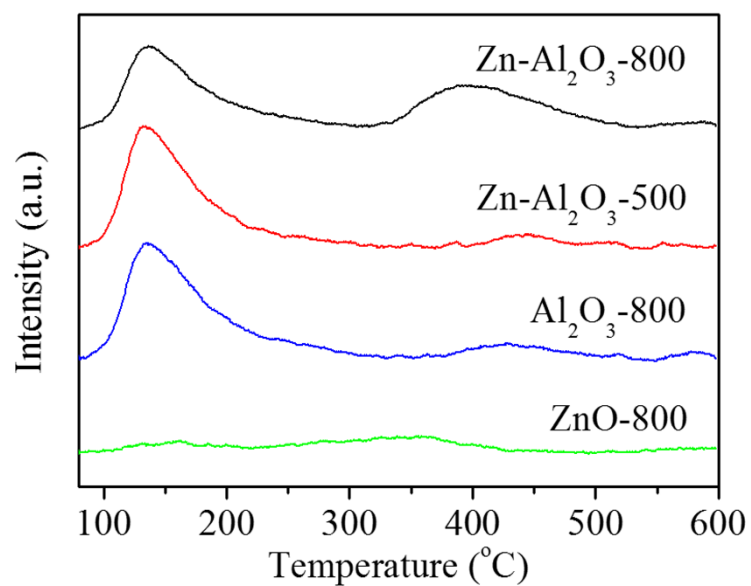


Fig. S14. CO₂-TPD profiles of Zn-Al₂O₃-800, Zn-Al₂O₃-500, Al₂O₃-800, and ZnO-800.

Table S1 Activities of some catalysts for N₂O decomposition in reported literature

Catalyst	Mass of catalyst (g)	Active element content (wt%)	Flow rate (cm ³ min ⁻¹)	Gas composition	T ₅₀ (°C)	T ₉₀ (°C)	Reference
Rh/Zn-Al ₂ O ₃ -800	0.5	1.1	60	0.5% N ₂ O	251	271	this work
Rh/Zn-Al ₂ O ₃ -800	0.5	1.1	60	0.5% N ₂ O + 5% O ₂ + 2% H ₂ O	333	371	this work
Rh/Al ₂ O ₃	0.5	1.0	60	0.5% N ₂ O	289	318	this work
Rh/Al ₂ O ₃	0.5	1.0	60	0.5% N ₂ O + 5% O ₂ + 2% H ₂ O	388	421	this work
Rh/TiO ₂	0.5	1.0	60	0.5% N ₂ O	310	340	[24]
Rh/SiO ₂	0.5	1.0	60	0.5% N ₂ O	324	360	[24]
Rh/CeO ₂	0.5	1.0	60	0.5% N ₂ O	223	250	[26]
Rh/HAP-PEG-200	0.5	0.97	60	0.5% N ₂ O	223	245	[26]
Rh/HAP-PEG-200	0.5	0.97	60	0.5% N ₂ O + 5% O ₂ + 2% H ₂ O	344	386	[26]
Rh/USY	0.05	2.0	50	0.095% N ₂ O	237	258	[21]
Cu-ZSM-11	0.2	3.06	60	0.5% N ₂ O	348	373	[46]
Fe-ZSM-11	0.2	3.90	60	0.5% N ₂ O	435	465	[5]
Co-ZSM-11	0.2	3.59	60	0.5% N ₂ O	387	435	[51]
Pd/CeO ₂	0.1	0.5	100	0.1% N ₂ O	470	— ^a	[57]
Pt/CeO ₂	0.1	0.5	100	0.1% N ₂ O	462	— ^a	[57]
Ir/CeO ₂ -Al ₂ O ₃	0.1	0.5	150	0.1% N ₂ O	474	535	[58]

^a Conversion did not reach 90% under the reaction condition.